CHAPTER IV
RESULTS AND DISCUSSION

4.1 Ziegler-Natta Catalyst System: TiCl$_4$/MgCl$_2$ + Triethylaluminum (TEA)

4.1.1 Effect of Polymerization Temperature

Table 4.1 shows the effect of temperature on the polymerization reaction. The temperature was varied from 50-90 °C while ethylene pressure, catalyst, and cocatalyst concentrations were kept constant. When the polymerization temperature increases, polymer yield and productivity increase. This is because higher temperature induces more active Ti atoms. Marques et al. (1998) also reported that the active center concentration increases significantly with increase in temperature. However at 90 °C, both the yield and productivity start to decrease. The results show that catalyst active species may be decomposed when temperature exceeds 80 °C.

In contrast, the molecular weight (M_w) decreases with increasing temperature. Marques et al. (1993) suggested that the activation energy of the termination process is higher than that of the propagation process. Therefore when higher temperature is used, the rate of chain termination will increase leading to a decrease in the molecular weight.

Table 4.1 Effect of temperature on ethylene polymerization by Ziegler-Natta catalyst.

[Ti] = 0.0187 mmol/L, [Al] = 1.33 mmol/L, Al/Ti = 71.12, P_{Et} = 2 bar,
total volume = 150 ml in n-hexane, reaction time = 1 hr.

Entry	Temp	Yield (g)	Productivity (kg PE/mol Ti. atm. h)	T_m	X_c	M_n ($\times 10^4$)	M_w ($\times 10^4$)	MWD
47	50	7.99	1,427	131.03	53.07	-	-	-
46	60	10.73	1,916	130.03	52.05	16.5	83.4	5.05
45	70	11.43	2,041	130.03	51.60	17.7	73.4	4.15
44	80	14.94	2,668	129.53	50.28	18.1	73.5	4.07
50	90	4.88	871	128.87	49.47	6.9	40.3	5.80

Note : T_m and ΔH values were collected from second scan of DSC
%Crystallinity $(X_c) = (\Delta H / 290) \times 100$
M_n, M_w, MWD from GPC

In contrast, the molecular weight (M_w) decreases with increasing temperature. Marques et al. (1993) suggested that the activation energy of the termination process is higher than that of the propagation process. Therefore when higher temperature is used, the rate of chain termination will increase leading to a decrease in the molecular weight.

4.1.2 Effect of Triethylaluminum (TEA) Concentration and Al/Ti Ratio

Triethylaluminum $(Al(C_2H_5)_3)$ is the most widely used cocatalyst for Ziegler-Natta catalyst system. Varying TEA concentration with fixed catalyst concentration will also vary Al/Ti ratio. In this work, the TEA concentration was varied from 1.33-4.00 mmol/L with Al/Ti varied from 71.12 to 213.90. The results obtained are shown in Table 4.2.

Table 4.2 Effect of triethylaluminum concentration and Al/Ti ratio.

[Ti] = 0.0187 mmol/L, P_{Et} = 2 bar, T = 70 °C, reaction time = 1 hr

entry	Al/Ti	yield (g)	Productivity (kg PE/mol Ti. atm. h)	T_m	X_c	% Crystal-linity *	t ** (nm)	M_n (×10⁴)	M_w (×10⁴)	MWD
45	71.12	11.43	2,041	130.03	51.60	35.46	-	17.7	73.4	4.15
49	106.95	19.15	3,420	131.20	49.67	37.35	11.5	10.6	54.2	5.13
48	142.78	24.87	4,441	132.53	54.94	41.23	12.3	7.5	58.2	7.72
51	178.07	31.71	5,663	133.70	62.21	42.92	12.3	8.2	45.9	5.58
62	213.90	31.20	5,571	133.87	62.10	43.44	11.9	5.8	43.8	7.49

(*) : calculated from XRD results

(**) : crystallite size from XRD

The results show that polymer yield and productivity increase with increase in TEA concentration, because more Ti atoms are activated at high TEA concentration. This is supported by the work of Marques et al. (1998) who found that active center concentration increases when TEA concentration increases. However when Al/Ti ratio exceeds 200, the polymer yield seems to reach a constant value. This is because the excess amount of TEA may lead to an increase in the rate of chain transfer to alkylaluminum and this is confirmed by the decrease in molecular weight as Al/Ti ratio increases throughout the range of TEA concentration used in this work.

The trends of melting temperature and degree of crystallinity are inverse to the trend of molecular weight. This is because at very high molecular weight, the molecular weight itself does not have much effect on melting temperature and degree of crystallinity. The branching content is the key effect on them. Consequently their trends should be in the same direction as the trend of molecular weight distribution which is the case as shown in Table 4.2.

4.2 Metallocene Catalyst System:

Cp₂ZrCl₂ + Trialkylaluminum (TMA/TEA) +
### Tris(pentafluorophenyl) borane (B(C₆F₅)₃)

In this metallocene catalyst system, trialkylaluminum (AlR_3) was used as the alkylating agent for dichlorozirconocene catalyst (Cp_2ZrCl_2) to produce the cationic active species ($Cp_2ZrCH_3^+$). The highly active Lewis acid, tris(pentafluorophenyl)borane, was the alternative cocatalyst for metallocene in place of MAO. The catalyst injection into the reactor was in the order of metallocene, alkylaluminum, and $B(C_6F_5)_3$.

Table 4.3 shows the effect of TMA concentration and the presence of $B(C_6F_5)_3$ on the polymerization of polyethylene. The results show that in the absence of $B(C_6F_5)_3$, Cp_2ZrCl_2-TMA catalyst system [1] can initiate the polymerization reaction giving a small amount of polyethylene. The productivity increases with increase in Al/Ti ratio. This shows that dichlorozirconocene can be activated to polymerize polyethylene in the presence of only TMA. The mechanisms of methylation, methyl abstraction and monomer insertion in this case are demonstrated in Scheme 4.1.

Table 4.3 Effect of trimethylaluminum (TMA) concentration and $B(C_6F_5)_3$.

[Zr] = 2 μmol, P_{Et} = 2 bar, T = 30 °C, total volume = 150 ml in toluene, reaction time = 1 hr

Entry	[Al] (mmol)	Al/Zr	B(C₆F₅)₃ (μmol)	Yield (g)	Productivity (kgPE/molZr. atm.h)	T_m	X_c	M_n (×10⁴)	M_w (×10⁴)	MWD
14	0.4	200	-	0.056	14.0	-	-	-	-	-
2	1	500	-	0.250	62.5	134.00	77.28	3.0	38.2	12.62
1	2	1000	-	0.310	77.5	133.53	78.50	5.2	41.8	8.04
15	0.4	200	3	0.316	79.0	133.66	66.09	3.1	21.6	6.93
4	1	500	3	0.300	75.0	134.53	76.59	2.2	16.2	7.33
11	2	1000	3	0.314	78.5	133.00	44.93	3.0	40.6	13.42
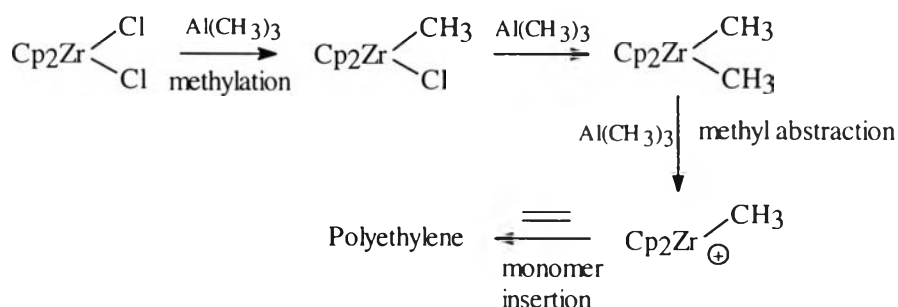
Scheme 4.1 Mechanism of ethylene polymerization by Cp_2ZrCl_2 – TMA.

In the presence of $B(C_6F_5)_3$, the Cp_2ZrCl_2-TMA-$B(C_6F_5)_3$ catalyst system [2] gives almost the same yield as system [1] at Al/Zr ratio ranging from 200-1000. It is interesting to note that at low Al/Zr of 200, the yield from system [2] is five times higher than [1]. This indicates that $B(C_6F_5)_3$ plays an important role in the increase of catalyst activity. However at higher Al/Zr ratio, the productivity of [2] is similar to [1]. This may be that at high TMA concentration, TMA plays a predominant role in polymerization even in the presence of $B(C_6F_5)_3$. Therefore at high Al/Zr ratio, either with or without $B(C_6F_5)_3$ in the catalyst system, the productivity is the same at the same TMA concentration.

The degree of crystallinity of system [2] at high Al/Zr = 1000 is only 45. This value is confirmed by the very board molecular weight distribution of 13. It is possible that there is a competition of TMA and $B(C_6F_5)_3$ in polymerization and the excess TMA leads to many branches on polyethylene molecules. The values of molecular weight distribution are rather broad compared to the typical MWD of about 2 of metallocene polyethylene. This may be due to the very low polymer yields resulting in the uneven chain termination throughout the system, therefore widely different molecular weight polyethylenes were obtained.

The effect of TMA concentration was studied and the results are shown in Table 4.4. When the TMA concentration increases, productivity also increases. This trend is similar to the Ziegler catalyst but with far less yield.

Table 4.4 Effect of trimethylaluminum (TMA) concentration.

[Zr] = 10 μmol, B/Zr = 1, P_{Et} = 2 bar, T = 20 °C, total volume = 150 ml in toluene, reaction time = 1 hr

Entry	[Al] (mmol)	Al/Zr	Yield (g)	Productivity (kgPE/molZr.atm.h)	T_{in}	X_c	M_n ($\times 10^4$)	M_w ($\times 10^4$)	MWD
7	0.5	50	0.290	14.5	-	-	-	-	-
22	0.6	60	0.356	17.8	133.87	77.01	3.5	31.9	9.03
23	0.8	80	0.610	30.5	134.17	68.27	5.5	37.3	6.73
27	1.0	100	0.948	47.4	134.20	66.66	7.1	41.1	5.75

The productivity of systems [1] and [2] was compared at Al/Zr ratio ranging from 0 to 1000 as shown in Figure 4.1. As described above, B(C$_6$F$_5$)$_3$ in the system helps to increase the productivity of system [2] but the productivity of both systems tend to come closer with increase in Al/Zr ratio.
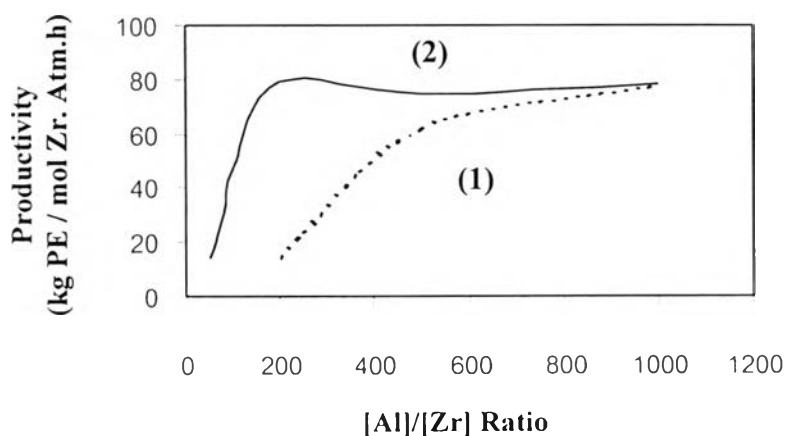
Figure 4.1 Productivity versus [Al]/[Zr] ratio of Cp$_2$ZrCl$_2$-TMA catalyst system [1] and Cp$_2$ZrCl$_2$-TMA-B(C$_6$F$_5$)$_3$ catalyst system [2].

However, the highest productivity of Cp_2ZrCl_2-TMA-$B(C_6F_5)_3$ catalyst system in this research is only 79, which is far less than $TiCl_4/MgCl_2$-TEA (2000-5000 kg PE/molZr.atm.h) and $Cp_2Zr(CH_3)_2$-$B(C_6F_5)_3$ catalyst system (3000-7000 kg PE/molZr.atm.h) as reported by Yang et al. (1991,1994).

4.3 Comparison of Properties of LDPE And Polyethylene From Ziegler-Natta and Metallocene Catalysts

4.3.1 Chain Branching from FT-IR Measurement

FTIR spectra of polyethylene are shown in Figure 4.2. The commercial low density polyethylene (LDPE) was tested by FTIR spectroscopy to compared with polyethylene produced by Ziegler-Natta and metallocene catalysts. The general absorption frequencies for polyethylene are listed in Table 4.5.

Table 4.5 Absorption frequency (cm^{-1}) of polyethylene.

Type	Absorption Frequency (cm^{-1})	Remarks
CH_3	2962	C-H Asymmetric Stretching
	2872	C-H Symmetric Stretching
	1450	C-H Asymmetric Bending
	1378	C-H Symmetric Bending
CH_2	2926	C-H Asymmetric Stretching
	2853	C-H Symmetric Stretching
	1465	C-H Symmetric Bending
	722	CH_2 Rocking

Figure 4.3 shows IR spectra in the range of 1320-1400 cm^{-1} which covers the absorption due to the methyl branches at 1378 cm^{-1}. Compared to LDPE, the polyethylene produced by Ziegler and metallocene catalysts shows no peak at 1378 cm^{-1}, while LDPE shows distinct C-H symmetric bending of – CH$_3$. This indicates that Ziegler and metallocene polyethylene is relatively linear with only a small amount of branches.
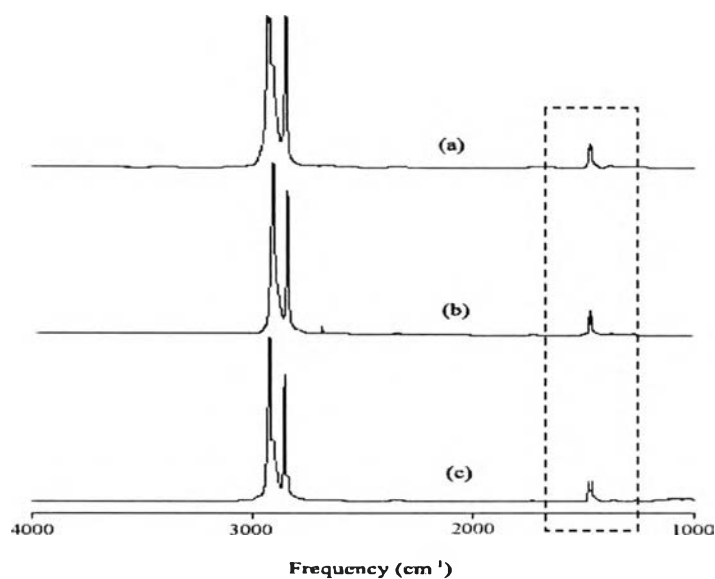
Figure 4.2 FTIR spectra of (**a**) commercial LDPE, (**b**) Ziegler-Natta polyethylene and (**c**) Metallocene
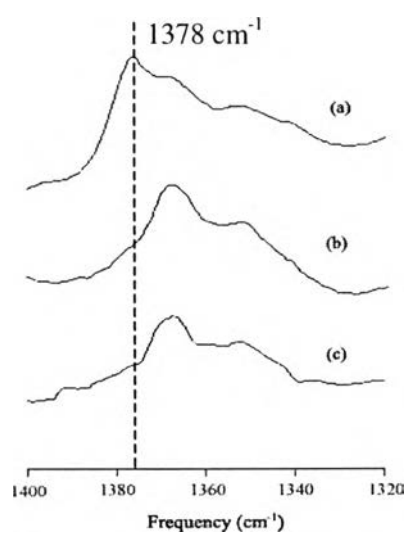
Figure 4.3 FTIR spectra of (**a**) LDPE, (**b**) Ziegler-Natta polyethylene, (**c**) Metallocene polyethylene in the range 1320-1400 cm^{-1}.

4.1.2 Crystallinity by X-Ray Diffraction

The degrees of crystallinity calculated from XRD results of polyethylene produced by Ziegler-Natta and metallocene catalysts are 35-45 and 40-60 respectively. Figure 4.4 shows the X-ray diffraction patterns of LDPE (%crystallinity = 32.8) compared to Ziegler and metallocene polyethylene. The two crystal diffraction peaks of metallocene polyethylene are bigger and sharper than those of Ziegler and LDPE.
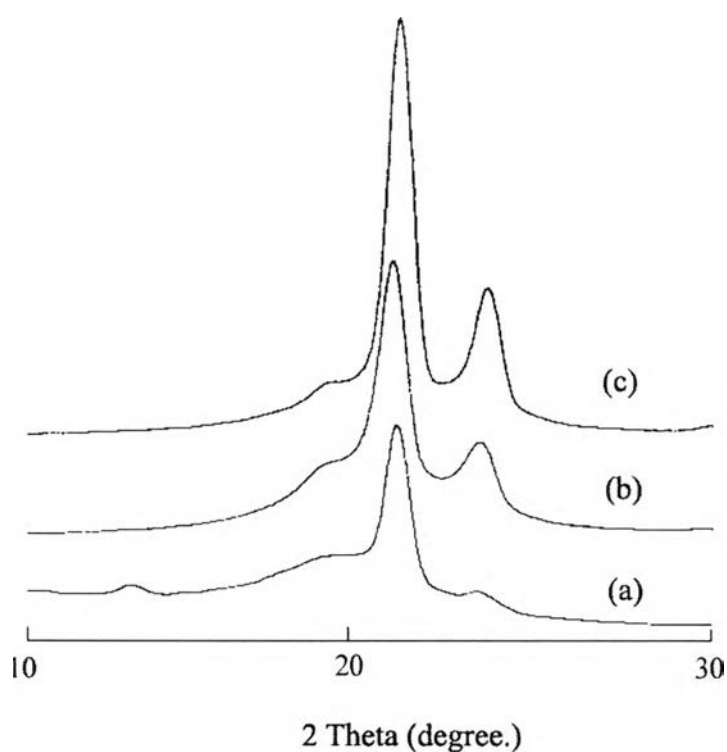

Figure 4.4 XRD patterns of polyethylene.

(a) LDPE, (b) Ziegler-Natta polyethylene, (c) Metallocene

4.3.3 Crystallinity from DSC

DSC characterization was operated from 50-160 °C with heating rate of 10 °C/min. The samples were then cooled down at the same rate then heated up again. The values of melting point and crystallinity were collected from the second scan to eliminate the polymerization history.

The DSC thermogram of metallocene polyethylene in Figure 4.5 shows higher area under melting peak than Ziegler polyethylene. This area is used to calculate the heat of fusion and the degree of crystallinity. The degree of crystallinity from DSC of Ziegler polyethylene is 49-62 while that of metallocene polyethylene is 66-78 at Al/Zr ratio below 500. The crystalline peak around 117 °C of metallocene polyethylene is also sharper than Ziegler polyethylene.
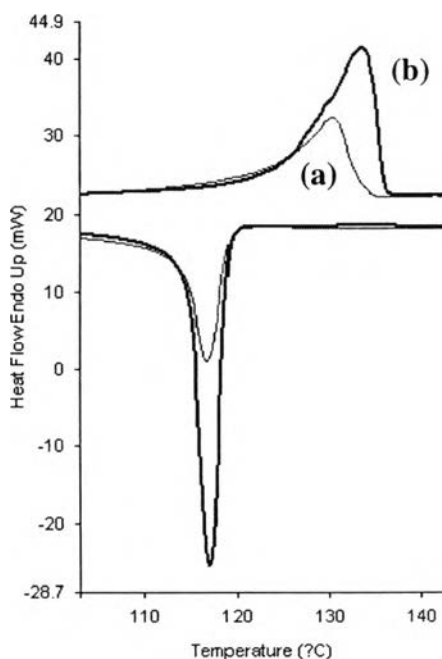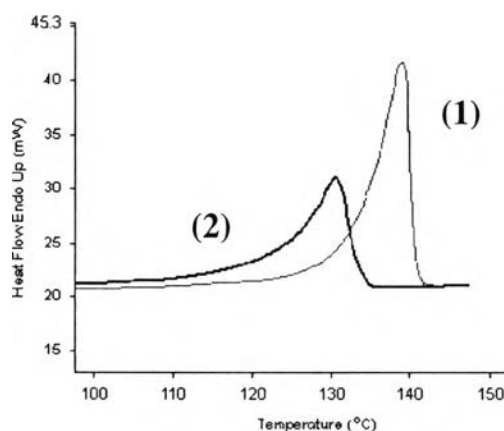

Figure 4.5 DSC thermogram of (a) Ziegler-Natta polyethylene and (b) metallocene polyethylene.

4.4 Morphology Study

4.4.1 Ziegler-Natta Polymerization

The first and second scans of DSC characterization were collected. As discussed previously, the first scan depends on the polymer morphology after polymerization, while the second scan after recrystallization at the same cooling rate depends on the polymer structure.

Figure 4.6 The DSC thermograms of first (1) and second (2) scan of Ziegler polyethylene.

Figure 4.6 shows the first and second scan DSC curves of polyethylene obtained from Ziegler-Natta catalyst system. The melting point and % crystallinity of the first and second scans are shown in Table 4.6. The values of the first scan are higher than those of the second scan. This indicates that the polymer morphology after polymerization process is better than after recrystallization.

This is because there are many $TiCl_4$ sites on a heterogeneous $MgCl_2$ support particle. When the polymerization occurs, these catalyst molecules will become active sites leading to many growing polymer chains on one

particle. These molecules are very close to each other and can pack together well (Fig. 4.7). This will result in the high melting point and % crystallinity when it is detected by first DSC scan.

Table 4.6 The melting temperature and degree of crystallinity of first and second scan of Ziegler polyethylene by DSC.

[Ti] = 0.0187 mmol/L, P_{Et} = 2 bar, T = 70 °C, reaction time = 1 hr

| entry	Al/Ti	yield (g)	Productivity (kg PE/mol Ti. atm. h)	T_c	$T_m^{[1]}$	$T_m^{[2]}$	$X_c^{[1]}$	$X_c^{[2]}$
62	213.90	31.20	5,571	116.87	138.83	133.87	76.87	62.10
51	178.07	31.71	5,663	117.09	138.70	133.70	71.84	62.21
48	142.78	24.87	4,441	116.83	140.03	132.53	69.28	54.94
49	106.95	19.15	3,420	117.10	139.53	131.20	67.59	49.67
45	71.12	11.43	2,041	116.30	138.67	130.03	64.51	51.60
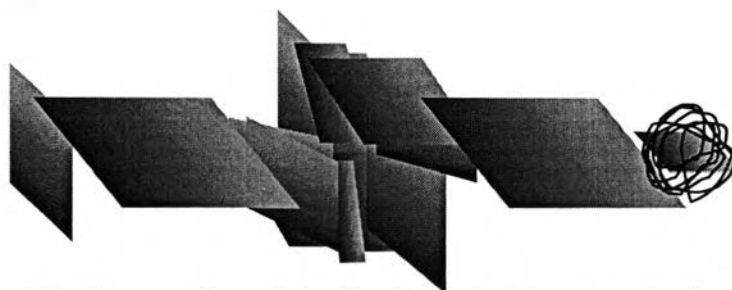
Figure 4.7 Proposed model of polymerization morphology of Ziegler-Natta catalyst (I).
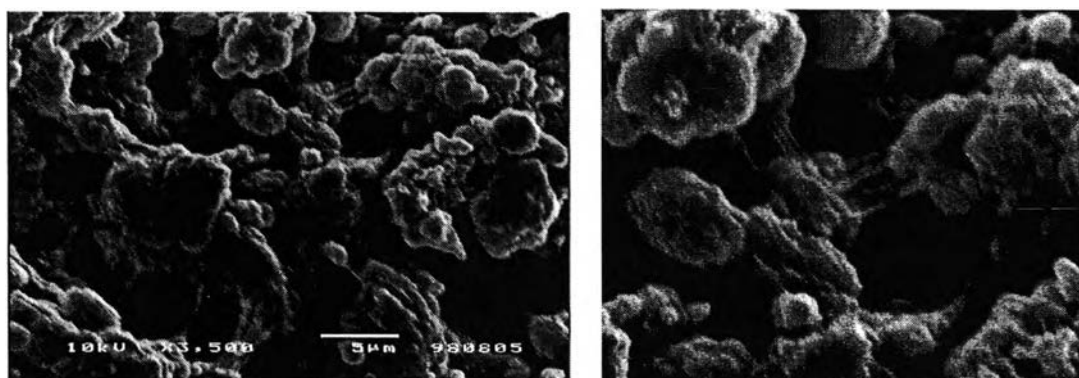
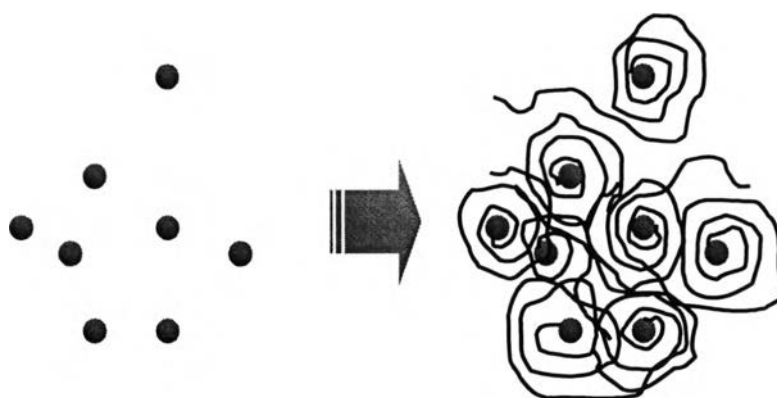**Figure 4.8** The SEM picture of Ziegler polyethylene.

The SEM picture of Ziegler polyethylene in Figure 4.8 shows the sphere-like polymer with fiber-like linkage. This is because the particles of catalyst consist of aggregates of small catalyst crystals. When the polymer is generated and continuously growing, the mechanical pressure will cleave out these aggregates. The catalyst break-up process will first occur at the surface and move toward the center of the particles. This will leave the fiber-like linkages between the sphere-like polymer particles (Fig. 4.9).
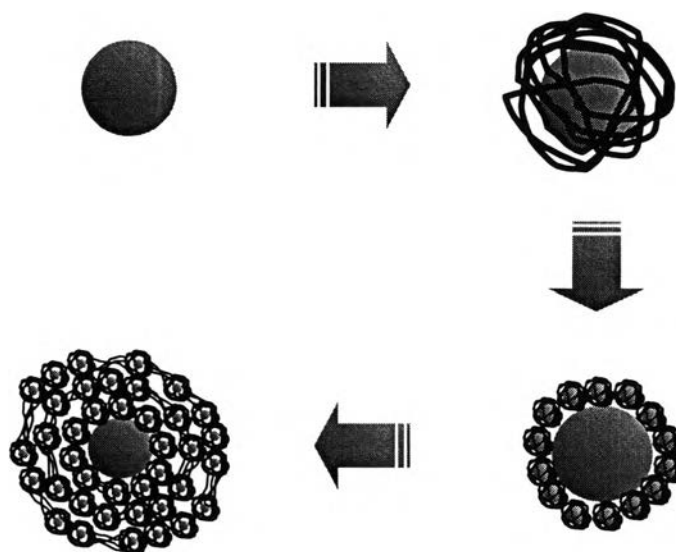

Figure 4.9 Proposed model of polymerization morphology of Ziegler-Natta catalyst (II).

4.4.2 Metallocene Polymerization

In contrast to heterogeneous Ziegler catalyst, metallocene catalyst will generate the homogeneously disperse active sites throughout the solution. When the polymerization occurs, each polymer chain will grow individually (Fig. 4.10). The morphology of the polyethylene product is therefore homogeneous as detected by SEM (Fig. 4.11).

**Figure 4.10** Proposed model of polymerization morphology of metallocene catalyst.
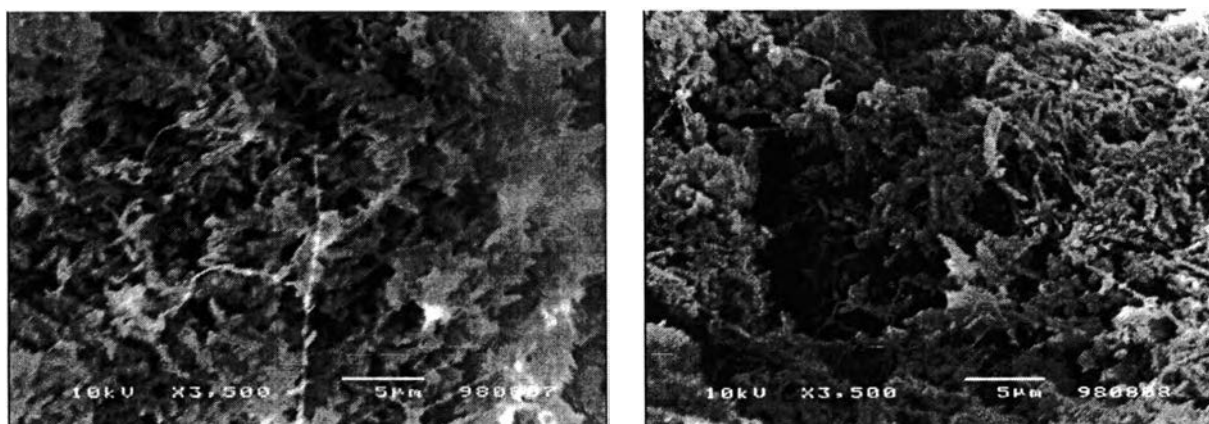
Figure 4.11 The SEM picture of metallocene polyethylene.

The melting temperatures of metallocene polyethylene from the first and second DSC scans are shown in Table 4.7 and Figure 4.12. The melting temperature of the first scan is higher than the second scan. The very low polymer yield indicates that there is a small amount of active sites generated in the solution. These active sites will polymerize ethylene individually and they do not pack well with neighboring chains. This results in the low melting point of the first scan.

Table 4.7 The melting temperature and degree of crystallinity of first and second scan of metallocene polyethylene by DSC.

[Zr] = 2 μmol/L, P_{E_1} = 2 bar, T = 30 °C, toluene

entry	Al/Zr	B(C_6F_5)$_3$ (μmol)	yield (g)	T_C	$T_m^{[1]}$	$T_m^{[2]}$	X_c
14	200	-	0.056	-	-	-	-
2	500	-	0.250	117.04	131.70	134.00	77.28
1	1000	-	0.310	117.42	130.37	133.53	78.50
15	200	3	0.316	117.85	133.00	133.66	66.09
4	500	3	0.300	116.56	132.83	134.53	76.59
11	1000	3	0.314	115.77	131.37	133.00	44.93
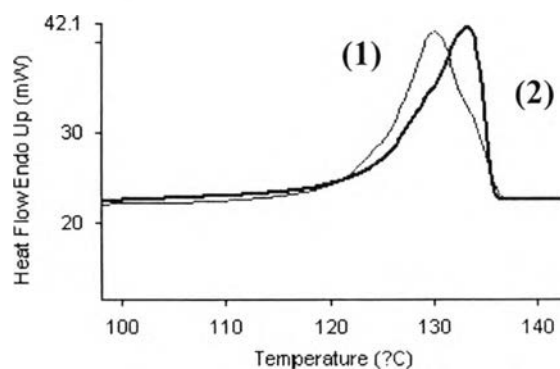
Figure 4.12 The DSC thermograms of first (1) and second (2) scans of metallocene polyethylene.

After polymerization, metallocene catalyst system gives swollen polyethylene in solution while Ziegler catalyst gives polyethylene particles at the bottom of the reactor (Fig. 4.13).

Ziegler polyethylene   Metallocene polyethylene
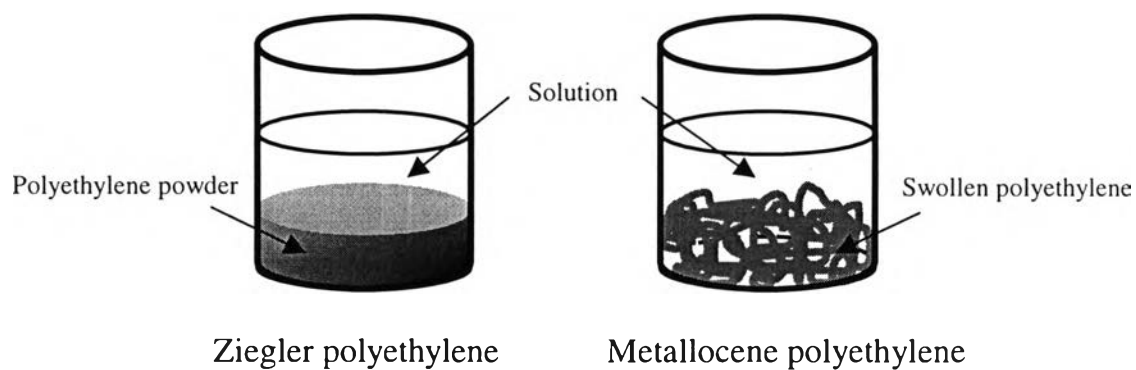
Figure 4.13 The model of the Ziegler and metallocene polyethylenes in the reactor after polymerization.